JACS
JOURNAL OF THE AMERICAN CHEMICAL SOCIETY

Article

pubs.acs.org/JACS

Method for Cellular Imaging of Palmitoylated Proteins with Clickable Probes and Proximity Ligation Applied to Hedgehog, Tubulin, and Ras

Xinxin Gao and Rami N. Hannoush*

Department of Early Discovery Biochemistry, Genentech, Inc., 1 DNA Way, South San Francisco, California 94080, United States

Supporting Information

ABSTRACT: Hedgehog protein undergoes post-translational palmitoylation, which is critical for its signaling activity during embryonic development and in adult tissues. Due to a lack of suitable imaging methods, the trafficking route of palmitoylated Hedgehog has remained unclear in secretory cells. Here, we report a novel method for imaging the subcellular distribution of palmitoylated forms of cellular proteins with high resolution. The method utilizes clickable chemical reporters to label the entire palmitoylated proteome, followed by proximity ligation on antibodies to the click-conjugated dye and the protein of interest to reveal the spatial localization of specific palmitoylated proteins, as exemplified by sonic Hedgehog, tubulin, and Ras. Palmitoylated sonic Hedgehog is found in the endoplasmic reticulum, the Golgi apparatus, and at the plasma membrane but not the endosomal system in Hedgehog-secreting cells. Palmitoylated tubulin is found along microtubule tracks and also partially associated with the plasma membrane, while palmitoylated H-Ras is visualized at various cellular locations including the plasma membrane, Golgi apparatus and endoplasmic reticulum. Our method is broadly applicable to imaging the palmitoylation of cellular proteins as well as other protein post-translational modifications that are detectable by clickable chemical reporters.

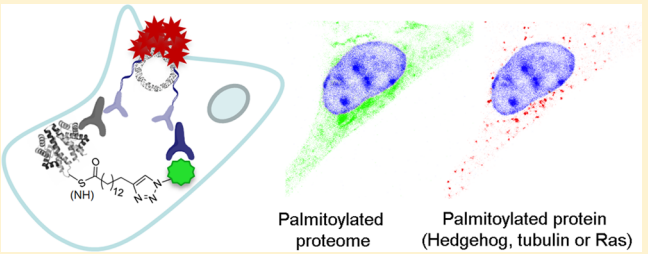

INTRODUCTION

Hedgehog (Hh) signaling is a key regulator of growth and patterning during embryonic development.[1] However, misregulation of Hh signaling via activating mutations has been linked to human disease such as basal cell carcinoma, medulloblastoma,[1,2] and via overexpression of Hh ligand in ovarian, pancreatic, lung, and colorectal cancers.[3] The signaling activity of Hh ligands is tightly regulated by their post-translational modifications. In cells, Hh is synthesized as a precursor protein that undergoes autoprocessing to generate an N-terminal fragment, which is modified with a cholesterol moiety via an ester bond at its C-terminus, and a palmitate group via an amide linkage at its N-terminus.[4,5] These hydrophobic modifications of Hh are believed to modulate its association with membranes and are essential for full activity of the ligand, enabling interaction with the receptor Patched and triggering activation of the downstream Gli zinc-finger transcription factor.[1]

It has been proposed that protein palmitoylation plays a vital role in Hh trafficking. However due to a lack of methods for visualizing the palmitoylated form of individual proteins, the transport routes of palmitoylated Hh in secretory cells have remained unclear. Recent methods have focused on biochemical detection of palmitoylated Hh in cellular lysates[6,7] and demonstrated its association with cellular membrane fractions.[6] Despite offering a robust and sensitive readout on the palmitoylation status of Hh, these biochemical methods fall short of deconvoluting the spatial localization of palmitoylated Hh in intact cells. Here, we report the development of a sensitive fluorescence imaging method that utilizes a clickable palmitic acid probe in combination with in situ proximity ligation, thereby enabling high resolution imaging of the palmitoylated form of Hh proteins and revealing their subcellular distribution. Proximity ligation has been used in the past by several groups for detecting protein−protein interactions,[8] but to our knowledge, this is the first demonstration of its use with clickable modifications of specific proteins.

Our click chemistry−proximity ligation method is broadly applicable to imaging the subcellular distribution of other palmitoylated proteins. As a test case, we adapted the method to gain insight into the spatial distribution of palmitoylated tubulin. Tubulin is a heterodimeric protein that constitutes the core building block of microtubules, which are present throughout the cell. Earlier biochemical studies demonstrated that tubulin undergoes post-translational palmitoylation in human platelets, leukemic lymphocytes and neuronal cell lines.[9−12] By using subcellular fractionation techniques coupled with radioactivity, a few groups reported that a fraction of palmitoylated tubulin is found in both cytoplasmic and membrane preparations.[9,13−15] Yet, whether palmitoylated

Received: October 7, 2013
Published: February 28, 2014

   dx.doi.org/10.1021/ja410068g | J. Am. Chem. Soc. 2014, 136, 4544−4550

tubulin is really present at the plasma membrane in intact cells remains unclear. Using our imaging method, we demonstrate that a small population of palmitoylated tubulin seems associated with the plasma membrane.

In another test case, we illustrated the applicability of our click chemistry–proximity ligation method to image the spatial localization of palmitoylated Ras, a protein which plays a key role in cell growth and division and is frequently mutated in cancer. The Ras isoform H-Ras undergoes post-translational palmitoylation as it traffics through the secretory pathway; of note is that palmitoylation of H-Ras is dynamic.[16−18] Cycles of palmitoylation and depalmitoylation on H-Ras regulate the protein's association with different compartments of the endomembrane system such as the endoplasmic reticulum (ER), Golgi, endosomes, and plasma membrane, thereby controlling its activity and function.[18−22] Despite these earlier groundbreaking studies which relied on protein overexpression and site-directed mutagenesis approaches, methods to image the palmitoylated form of endogenous H-Ras have been lacking. Here, by using a click chemistry–proximity ligation approach, we visualize palmitoylated H-Ras and observe its association with the ER, Golgi apparatus and plasma membrane. Finally, our imaging method enables further investigation into the spatial localization and steady-state distribution of endogenous palmitoylated H-Ras proteins under different cellular conditions and can be applied to imaging the palmitoylation of other cellular proteins.

RESULTS AND DISCUSSION

Method for Visualizing Hh Protein Palmitoylation. Our strategy utilized clickable chemical reporters and proximity ligation to detect palmitoylation on Hedgehog proteins in single cells (Figure 1). First, we incubated human embryonic kidney (HEK) 293 cells stably expressing sonic Hedgehog (Shh) with ω-alkyne palmitic acid (Alk-C16), a chemical reporter of global protein palmitoylation.[6,23,24] After cells were fixed and detergent-permeabilized, the alkyne-labeled palmitoylated proteins underwent a Cu^{1}-catalyzed Huisgen 1,3-dipolar cycloaddition reaction[25] with exogenously added azide-conjugated Oregon Green488 dye (Figure 1, step 1). This step enabled visualization of the palmitoylated proteome in intact cells. We then treated these cells with primary antibodies that specifically recognize the protein of interest (Shh in this case) and Oregon Green488. To visualize palmitoylated Shh, the cells were incubated with distinct secondary antibodies conjugated to complementary oligonucleotides that would hybridize to form a closed circle only when the two antibodies are in close proximity (<40 nm;[26] Figure 1, step 2). A subsequent rolling-circle amplification reaction coupled with hybridization of exogenously added fluorescently labeled oligonucleotides (Figure 1, step 3) was performed to amplify and visualize the proximity-dependent signal (i.e., palmitoylated Shh), which could be detected only when both primary antibodies were present (Figure 2), thereby validating the specificity of the assay.

Optimization of the palmitoylated Shh signal was achieved by systematically varying the primary antibody concentrations in a 96-well plate format. An excellent signal-to-background ratio was observed when using anti-Shh and anti-Oregon Green488 antibodies at the optimal concentrations of 4 and 10 μg/mL, respectively (Figure 2A). Notably, palmitoylated Shh was visualized in HEK293-Shh, but not in wild-type HEK293 cells which do not express endogenous Shh, indicating the assay

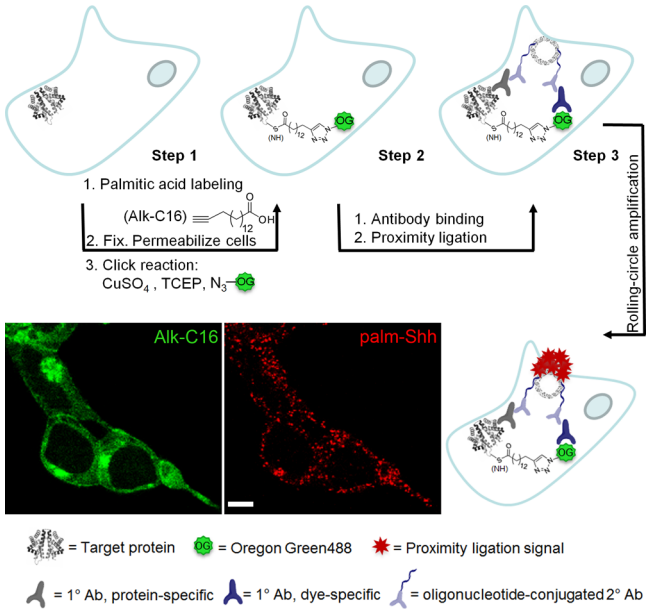

Figure 1. Click chemistry–proximity ligation method for visualizing palmitoylated cellular proteins. Cells were metabolically labeled with ω-alkyne palmitic acid (Alk-C16), fixed, detergent-permeabilized, and then processed for click reaction with azide-conjugated Oregon Green488 (step 1). After washing, cells were incubated with primary antibodies that specifically recognize the target protein and Oregon Green488 and were then processed for proximity ligation (steps 2 and 3) as described in methods. Images of palmitoylated Shh (red) and the total palmitoylated proteome (green) in HEK293-Shh cells are shown. Cells were imaged by a laser scanning confocal microscope using a 63× oil objective. Representative images from at least three independent experiments are shown. Ab, antibody. Scale bar, 5 μm.

readout is specific to Shh palmitoylation (Supporting Information, Figure 1). Moreover, palmitoylated Shh was observed in regions stained with total Shh protein (Figure 3A and Supporting Information, Figure 2). The reason that only a fraction of total Shh appears to be palmitoylated is likely because Shh turnover is slower than our palmitate metabolic labeling period. Due to the irreversible nature of the palmitate amide linkage on Shh, only newly synthesized proteins are labeled with Alk-C16. Our imaging data seem consistent with prior biochemical findings demonstrating that only a fraction of Shh is labeled with Alk-C16.[6]

Quantitative comparison of the proximity ligation (i.e., palmitoylated Shh) and immunofluorescence (i.e., total Shh) signals is not possible due to the nonlinearity of the proximity ligation signal. Furthermore, the total Shh signal is obtained by carrying out immunofluorescence against anti-Shh antibody that has already been bound to a secondary antibody as part of developing the proximity ligation signal (Figure 3A and Supporting Information, Figure 2), and this may lead to underrepresented signal of total Shh protein. Notwithstanding these limitations, the method has the utility for reporting the subcellular localization of a specific palmitoylated protein.

Palmitoylated Shh Associated with the ER-Golgi System but Not the Endosomal Network. Palmitoylated Shh was visualized in intracellular objects throughout the cytoplasm and at the plasma membrane, but not in the nucleus (Figure 1 and 3A and Supporting Information, Figure 2). To further investigate the cellular localization of palmitoylated Shh, we performed our imaging method in combination with

dx.doi.org/10.1021/ja410068g | J. Am. Chem. Soc. 2014, 136, 4544−4550

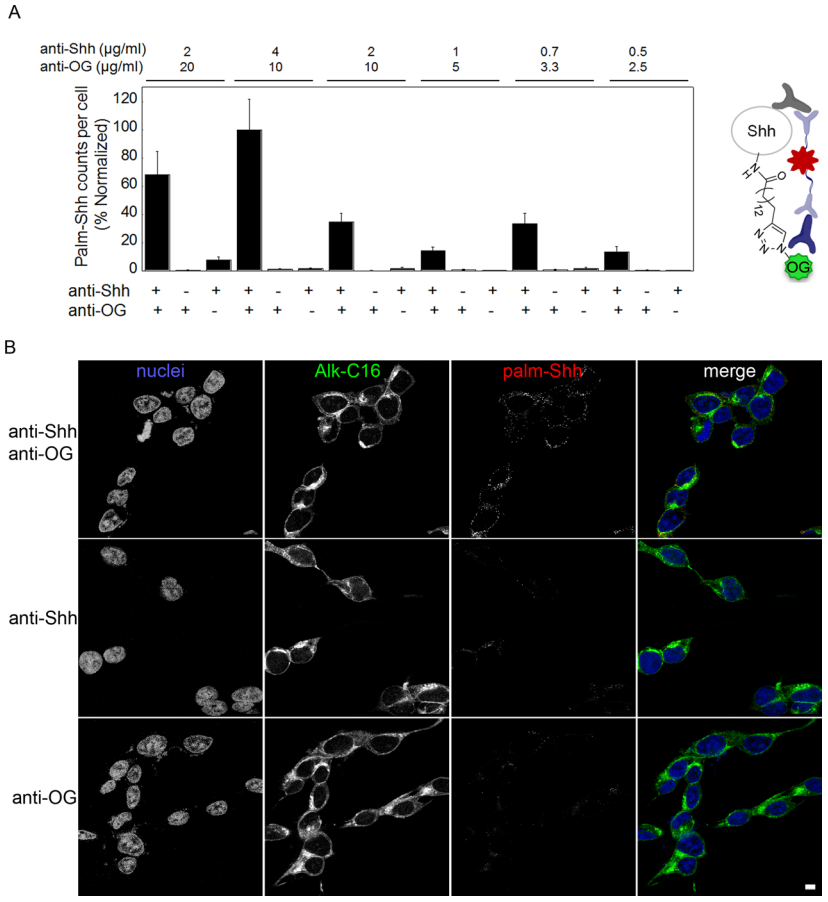

Figure 2. Cellular imaging of palmitoylated Shh. (A) Optimization of the assay for fluorescence imaging of Shh palmitoylation. A range of anti-Shh and anti-Oregon Green488 (OG) primary antibody concentrations was tested in HEK293-Shh cells plated in 96-well plates. Images were acquired on a high throughput ImageXpress Micro system using a 40× objective (mean ± SEM, n = 700 cells per condition). Spots corresponding to palmitoylated Shh were counted that are above a background threshold, which was set based on anti-OG antibody negative control (10 μg/mL, eighth column from left). Values were normalized to the condition with highest palm-Shh values (4 μg/mL anti-Shh and 10 μg/mL anti-Oregon Green488). (B) The assay readout is specific to palmitoylated Shh, requiring the presence of both anti-Shh and anti-OG antibodies. HEK293-Shh cells were metabolically labeled with Alk-C16, followed by click chemistry with azide-conjugated Oregon Green488, and processed for proximity ligation as described in methods. Anti-Shh (4 μg/mL) and anti-Oregon Green488 (10 μg/mL) antibodies were used. Cells were imaged by a laser scanning confocal microscope using a 63× oil objective. Representative data from at least three independent experiments are shown. Scale bar, 5 μm.

immunofluorescence against various cellular organelle markers. In this context, azide-conjugated biotin was used in the click reaction instead of Oregon Green488 to enable imaging of organelle markers in the FITC channel. In HEK293-Shh cells, there was no overwhelming pattern of palmitoylated Shh colocalization with any of the cellular markers examined. A fraction of palmitoylated Shh was found in the ER and Golgi, as shown by its partial colocalization with the ER marker CellLight ER-GFP and the *cis*-Golgi matrix protein marker GM130 (Figure 3B and Supporting Information, Figure 3−4). Also a subpopulation of palmitoylated Shh appeared to be at the plasma membrane as indicated by its partial association with the plasma membrane marker wheat germ agglutinin (Figure 3B and Supporting Information, Figure 5). Our data is consistent with a model in which Shh palmitoylation occurs in the luminal compartments along the secretory pathway (likely the ER), consistent with the reported localization of Hhat, the acyltransferase that regulates Hh palmitoylation, to the ER and/or the Golgi apparatus.[27]

Next, we investigated whether palmitoylated Shh is targeted to the endosomal network. In contrast to its Golgi and ER presence, palmitoylated Shh showed minimal apparent association with the early endosome marker Rab5a-GFP, the late endosome marker Rab7a-GFP, and the late endosome/lysosome marker, lysosome-associated membrane protein 1 (LAMP1)-GFP (Figure 4). Collectively, our findings suggest that palmitoylated Shh is transported through the ER-Golgi secretory pathway to the plasma membrane, circumventing endosomes and lysosomes, as is typical for secreted proteins. It remains to be determined whether palmitoylated Shh transport to the plasma membrane originates directly from the Golgi apparatus or goes through a yet unidentified post-Golgi compartment.

Visualization of Palmitoylated Tubulin. To assess whether the click chemistry−proximity ligation method could be readily adaptable to visualizing palmitoylation of other cellular proteins, we probed palmitoylation of endogenous α-tubulin. Mouse fibroblast L cells were treated with Alk-C16, fixed, and incubated with azide-tagged Alexa488 to reveal the palmitoylated proteome. Proximity ligation was then performed by using antibodies against α-tubulin and Alexa488. As expected, a signal corresponding to palmitoylated α-tubulin was detected only in cells that were incubated with both primary antibodies (Figure 5A and Supporting Information,

dx.doi.org/10.1021/ja410068g | J. Am. Chem. Soc. 2014, 136, 4544−4550

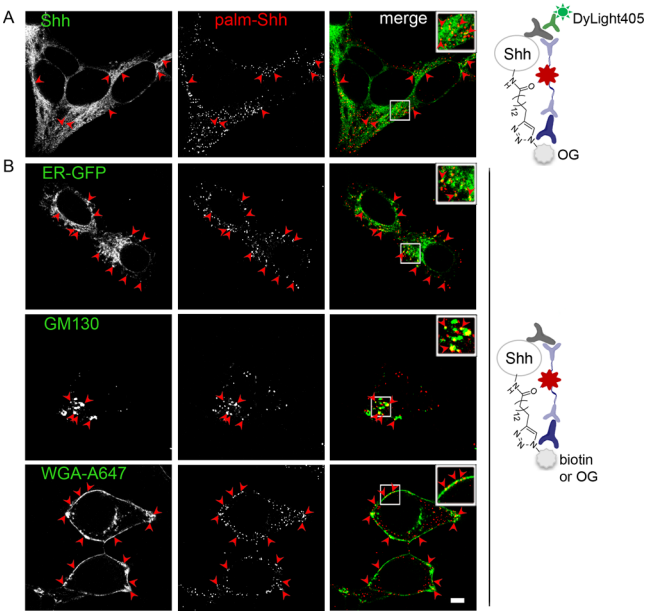

Figure 3. Subpopulation of palmitoylated Shh associated with the ER and Golgi in Shh-secreting cells. (A) Cellular distribution of palmitoylated Shh and total Shh in HEK293-Shh cells. DyLight405-conjugated anti-rabbit secondary antibody was used to detect Shh signal (shown in green, false colored). (B) A subpopulation of palmitoylated Shh was found in various cellular compartments including ER (marked with ER signal sequence of calreticulin and KDEL fused to GFP), the Golgi apparatus (marked with GM130) and the plasma membrane (marked with wheat germ agglutinin WGA conjugated to Alex647; shown in green, false colored). HEK293-Shh cells were processed for click chemistry with Oregon Green488 (for WGA staining) or biotin azide (for ER-GFP and GM130 staining) followed by proximity ligation and immunofluorescence as described in methods. Biotin-azide was used in the click reaction to enable fluorescence imaging of cellular organelle markers in the FITC channel (green). Representative images from two independent experiments are shown. Red arrows indicate representative examples of colocalization. Scale bar, 5 μm.

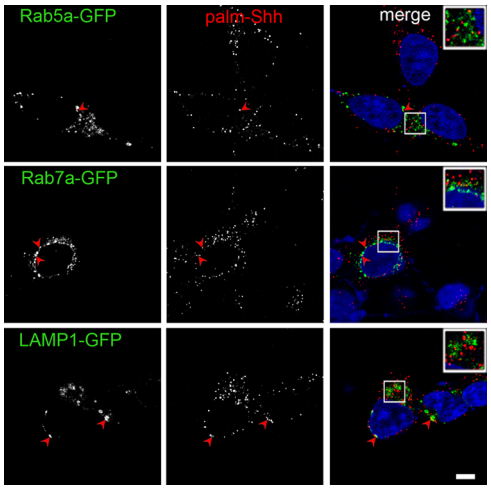

Figure 4. Palmitoylated Shh not associated with the endosomal network. Minimal association of palmitoylated Shh is observed with endosomal markers Rab5a-GFP (early endosome), Rab7a-GFP (late endosome), or LAMP1-GFP (late endosome/lysosome). HEK293-Shh cells were processed for click chemistry followed by proximity ligation and immunofluorescence as described in methods. Biotin-azide was used in the click reaction to enable fluorescence imaging of cellular organelle markers in the FITC channel (green). Representative images from two independent experiments are shown. Scale bar, 5 μm.

Figure 6). The use of azide-conjugated Alexa488 demonstrates that our imaging method is compatible with multiple fluorophores.

Treatment with vinblastine, a broad-spectrum chemotherapeutic agent shown earlier to inhibit tubulin palmitoylation,[10,11] led to a decrease (~65%) in the levels of palmitoylated α-tubulin with no apparent effect on palmitoylated proteome levels (Figure 5B,C). In contrast, the general acyltransferase inhibitor 2-bromopalmitic acid (BPA) reduced the levels of both palmitoylated α-tubulin and the palmitoylated proteome (Supporting Information, Figure 7). These findings highlight the specificity of our click chemistry–proximity ligation imaging method in reporting the palmitoylation status of an individual cellular protein, exemplified here by α-tubulin, and the total proteome simultaneously. Since tubulin may exist in macromolecular complexes, there may be a potential risk of signal artifacts due to proximity ligation between a palmitoylated tubulin protein and the epitope for a second tubulin protein that lies within the approximately 40 nm distance range of detection. While this scenario is possible in the case of tubulin, our palmitoylation inhibition data with vinblastine are consistent with earlier biochemical findings[11] and further validate the specificity of the tubulin palmitoylation signal detected in our click chemistry–proximity ligation assay.

The mechanism of how vinblastine inhibits tubulin palmitoylation remains unclear. We postulate that disrupting microtubule dynamics, by inhibition of tubulin polymerization, alters tubulin localization and hence accessibility to cellular palmitoyl acyltransferases, thereby inhibiting palmitoylation. Further studies are still needed to determine the extent, if any, to which loss in tubulin palmitoylation contributes to triggering apoptosis, and our method has the potential to enable such investigations.

Subcellular Localization of Palmitoylated α-Tubulin. In an effort to resolve the spatial distribution of the palmitoylated form of α-tubulin, we performed click chemistry with azide-tagged Alexa488 in Alk-C16-labeled mouse L cells. Proximity ligation was first performed to reveal the distribution of the palmitoylated form of α-tubulin, followed by immunofluorescence to detect total α-tubulin (Figure 5D,E). Total α-tubulin staining showed a meshwork-like structure of microtubules distributed throughout the cytoplasm, and a fraction of palmitoylated α-tubulin seemed to be associated with microtubule tracks (Figure 5E and Supporting Information, Figure 8). Furthermore, a small fraction of palmitoylated α-tubulin appeared to be at the plasma membrane (Figure 5F and Supporting Information, Figure 9), suggesting that this pool of palmitoylated tubulin is likely at the microtubule tips. However, there is still a large population of palmitoylated tubulin that did not appear to be associated with the plasma membrane, and our technique enables further investigation into its subcellular localization and the role that palmitoylation might play in tubulin membrane localization.

Visualization of Palmitoylated Ras. As an additional example to demonstrate the utility of the click chemistry - proximity ligation approach in detecting cellular proteins other than those which are overexpressed (such as Shh) or abundant (such as tubulin), we applied our method to image palmitoylation of endogenous H-Ras. In this regard, HeLa cells were metabolically labeled with Alk-C16, fixed, and

dx.doi.org/10.1021/ja410068g | J. Am. Chem. Soc. 2014, 136, 4544–4550

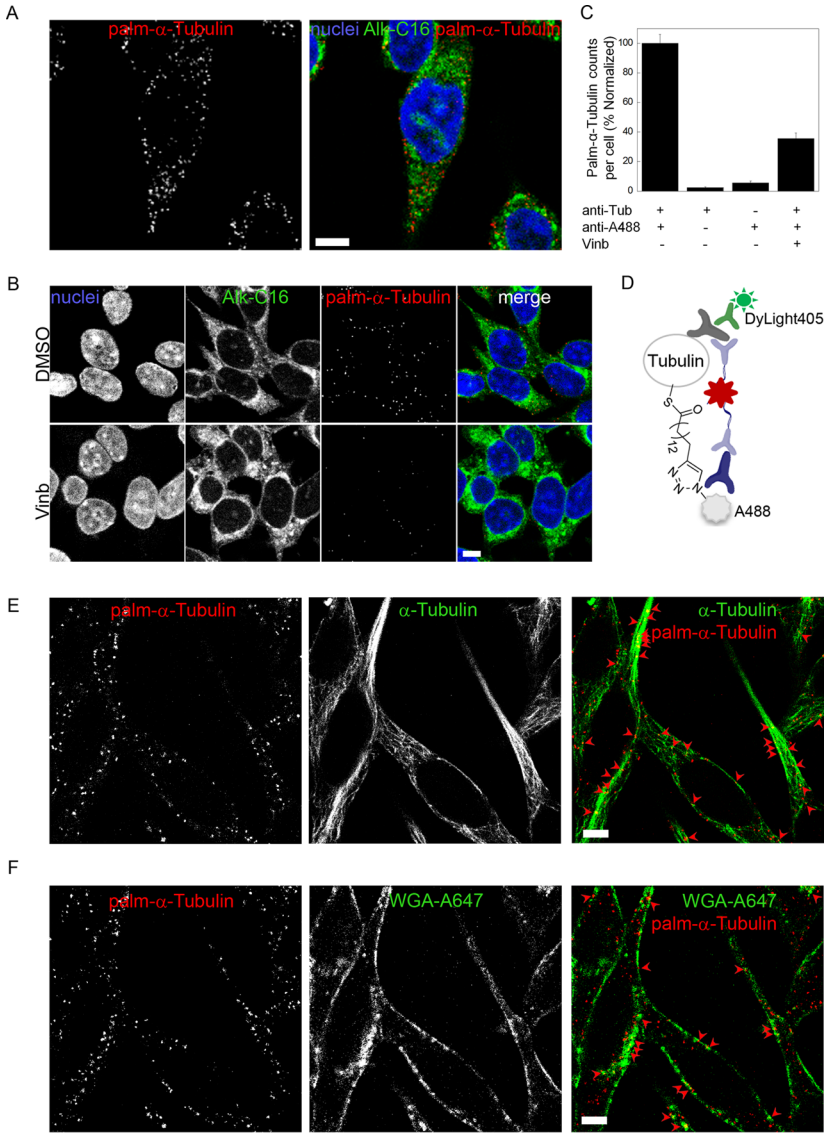

Figure 5. Fraction of palmitoylated α-tubulin appearing at the plasma membrane and along microtubules. (A) Simultaneous cellular imaging of palmitoylated α-tubulin and the palmitoylated proteome in mouse L cells. (B) Treatment (overnight) with vinblastine (Vinb, 1 μM) led to inhibition of α-tubulin palmitoylation in mouse L cells. Representative images are shown from three independent experiments. (C) Quantitation of palmitoylated α-tubulin spots per cell from experiments in (B). Either anti-α-tubulin or anti-Alexa488 (A488) antibodies were used as negative controls for the proximity ligation signal. Spots corresponding to palmitoylated α-tubulin were counted that are above a background threshold, which was set based on anti-α-tubulin antibody negative control sample. Values were normalized to the control anti-α-tubulin and anti-A488 sample, and represent mean $\pm$ SEM, n = 40–90 cells per condition. The graph is a representative of three independent experiments. (D) Schematic of the click chemistry–proximity ligation imaging strategy for both palmitoylated α-tubulin and total α-tubulin. (E) Subcellular distribution of total α-tubulin and palmitoylated α-tubulin. DyLight405-conjugated anti-mouse secondary antibody was used to detect α-tubulin signal (false colored as green). Red arrows indicate examples of sites where palmitoylated α-tubulin appears to be present along microtubules. (F) Partial association of palmitoylated α-tubulin with the plasma membrane marked by Alexa647-conjugated WGA (false colored as green). Red arrows indicate examples of sites where palmitoylated α-tubulin appears to be present at the plasma membrane. Cells were imaged by a laser scanning confocal microscope using a 63× oil objective. Images in panels E and F are from the same sample which was stained with both DyLight405-conjugated anti-mouse secondary antibody (for microtubule staining) and Alexa647-conjugated WGA (for plasma membrane staining); the images were acquired at different optical planes to capture the protein distribution along microtubules (E) and at the plasma membrane (F), respectively. Representative images from at least two independent experiments are shown. Scale bar, 5 μm.

processed for click reaction with azide-conjugated biotin. The cells were then incubated with anti-biotin and anti-H-Ras antibodies, followed by proximity ligation to yield the palmitoylated H-Ras signal (Figure 6A). Optimization of the antibody concentrations led to an excellent signal-to-background ratio (Supporting Information, Figure 10). We observed that a subpopulation palmitoylated H-Ras appeared to be distributed across the ER, Golgi apparatus, and, to a lesser extent, the plasma membrane (Figure 6B and Supplementary Figures 11–13). At this point, it cannot be ruled out that palmitoylated H-Ras might be present in other subcellular compartments such as the recycling endosomes,[22] and our imaging assay is ideal for assessing colocalization with these cellular compartments. Collectively, the above data further highlight the sensitivity of our method and illustrate its utility in

dx.doi.org/10.1021/ja410068g | J. Am. Chem. Soc. 2014, 136, 4544–4550

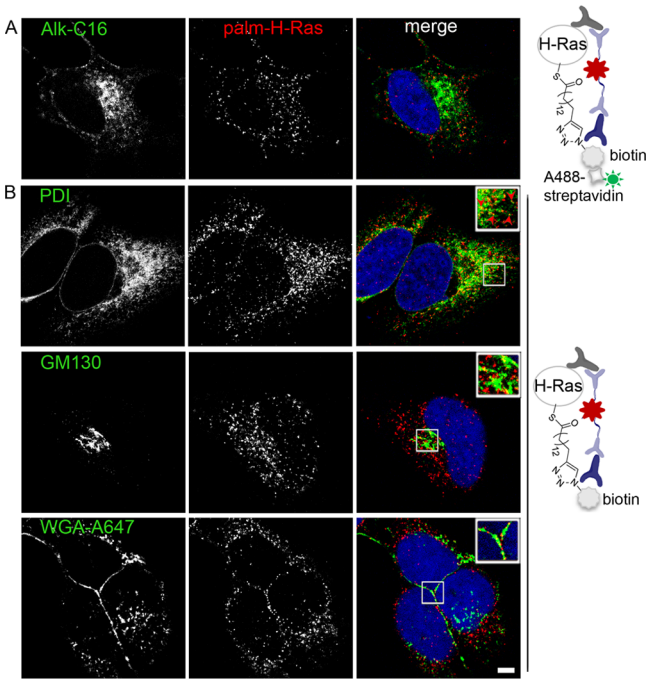

Figure 6. Visualization of palmitoylated H-Ras. (A) Simultaneous cellular imaging of palmitoylated H-Ras and total palmitoylated proteome in HeLa cells. Alexa488-conjugated streptavidin was used to detect the palmitoylated proteome (marked by Alk-C16). (B) A subpopulation of palmitoylated H-Ras was detected at the ER (marked with PDI, protein disulfide isomerase), Golgi apparatus (marked with GM130) and the plasma membrane (marked with WGA conjugated to Alex647; shown in green, false colored). HeLa cells were processed for click chemistry with biotin azide followed by proximity ligation and immunofluorescence as described in methods. Representative images from two independent experiments are shown. Red arrows indicate representative examples of colocalization. Scale bar, 5 μm.

labeling and detecting dynamically palmitoylated endogenous proteins as exemplified by H-Ras.

CONCLUSION

To date, methods that enable imaging the post-translationally palmitoylated form of cellular proteins have been lacking. Although proximity ligation has been used to detect protein–protein interactions,[8,26] we describe here a novel method for imaging specific palmitoylated proteins such as transfected Shh, endogenous α-tubulin, or H-Ras in single cells by using clickable palmitic acid probes and proximity ligation. Palmitoylated Shh was found distributed across the ER, Golgi, and plasma membrane, indicating that it is likely palmitoylated after translation in the ER and follows a typical secretory route to the cell surface. A fraction of palmitoylated α-tubulin was found along microtubules and, to a lesser extent, at the plasma membrane, while palmitoylated H-Ras was detected at the ER, Golgi apparatus, and plasma membrane to a varying degree. We believe that click chemistry–proximity ligation will be a powerful tool for further dissecting the possible role of palmitoylation in regulating the spatial distribution of palmitoylated proteins,[28] and for advancing studies, for example, about the relationship between tubulin palmitoylation, microtubule organization and apoptosis in the context of human disease. Moreover, our imaging method has a broad application in visualizing the fatty acylation of other cellular proteins, and may even have utility in drug discovery for validating the mechanism of action of Hh acyltransferase inhibitors potentially useful in treating Hh-ligand-dependent cancers. Finally, we believe the combined use of click chemistry with proximity ligation offers a promising approach to image other protein co- or post-translational marks detectable by click chemistry-based reporters such as glycosylation, cholesterolation, methylation, acetylation, AMPylation, and sulfenation.

EXPERIMENTAL METHODS

Reagents and Cell Culture. ω-Alkynyl palmitic acid (Alk-C16) and biotin-azide were synthesized as described earlier.[23] Human embryonic kidney (HEK) 293 cells stably overexpressing Shh (Genentech), mouse fibroblast L cells (ATCC no. CRL-2648) or HeLa cells (ATCC no. CCL-2) were grown in high glucose Dulbecco's Modified Eagle's Medium (DMEM) supplemented with 10% fetal bovine serum (FBS), 0.4 mg/mL Geneticin (for HEK293-Shh cells only) and 2 mM Glutamax. All cells used were incubated in a 5% CO_2 humidified incubator at 37 °C for 24 h before any experiments. For infection with CellLight reagents (ER-GFP, Rab5a-GFP, Rab7a-GFP and LAMP1-GFP), cells were incubated with 1 mL medium containing 20 μL CellLight reagents for 8 h then labeled with Alk-C16 overnight on 18 mm coverslips. CellLight reagents, Alexa-647-conjugated WGA, Alexa488-conjugated anti-mouse secondary antibody, Alexa647-conjugated anti-rabbit secondary antibody, Alexa488-conjugated streptavidin, and azide-conjugated Alexa488/Oregon Green488/biotin were purchased from Life Technologies. DyLight 405-conjugated anti-mouse and anti-rabbit secondary antibodies were from Thermo Scientific. Duolink II reagents were purchased from Olink Bioscience. Vinblastine, 2-bromopalmitic acid, copper sulfate ($CuSO_4$), Tris(2-carboxyethyl)phosphine hydrochloride (TCEP), and Corning CellBIND 96-well plates (clear flat bottom, black) were purchased from Sigma-Aldrich. BioCoat poly-D-lysine 96-well microplates (black/clear) were purchased from BD Biosciences.

Metabolic Labeling of Palmitoylated Proteins.[6,23] Alk-C16 was dissolved in DMSO to a final stock concentration of 50 mM and diluted to a final concentration of 100 μM in DMEM supplemented with 5% BSA (fatty acid-free) or 10% FBS (for labeling HeLa cells). The Alk-C16-containing medium was sonicated for 15 min at room temperature and then allowed to precomplex for another 15 min. Cells were seeded onto glass coverslips on a 12-well culture plate (200,000 cells per well, for all cell lines), BioCoat Poly-D-Lysine 96-well microplates (5,000 cells per well, for HEK293-Shh cells), or Corning CellBIND 96-well plates (5,000 cells per well, for mouse L and HeLa cells), and incubated for 24 h before treatment. After removal of the growth medium, cells were washed once with PBS before addition of Alk-C16-containing medium (0.5 mL for coverslips and 100 μL per well for 96-well plates). After overnight incubation at 37 °C/5% CO_2, cells were washed three times with cold PBS and fixed with cold methanol at −20 °C for 10 min, then further permeabilized with 0.1% Triton X-100 in PBS at room temperature for 5 min. Fixed cells were washed three times with PBS and subjected to the click labeling reaction in a 100 μL volume for 1 h at room temperature at final concentrations of the following reagents:[23] 0.1 mM azide dye (Oregon Green488-azide and biotin-azide for HEK293-Shh cells, biotin-azide for HeLa cells, and Alexa488-azide for mouse L cells), 1 mM TCEP dissolved in water and 1 mM $CuSO_4$ in water.

Detection of Palmitoylated Hh, α-Tubulin, and H-Ras. Fixed cells labeled with azide-conjugated dye were washed extensively with PBS and incubated in blocking buffer (PBS/5% BSA/0.3% Triton X-100) for 1 h at room temperature. For immunofluorescence, cells were stained with mouse anti-GM130 (BD Biosciences, 610823, 1:50, 5 μg/mL), anti-PDI (Abcam, ab2792, 1:100, 10 μg/mL), or anti-GFP (Clontech, 632381, 1:1000, 1 μg/mL) antibodies and the appropriate secondary antibodies (1:500). To stain plasma membrane, WGA Alexa-647 (100 μg/mL) was added to live cells for 15 min then washed twice with medium. For detection of palmitoylated Shh, cells were incubated with 4 μg/mL rabbit anti-Shh H-160 (Santa Cruz Biotech, Sc-9024) overnight at 4 °C, washed with PBS/0.05% Tween-20 (PBS-T), and then incubated for 1 h at room temperature with

dx.doi.org/10.1021/ja410068g | J. Am. Chem. Soc. 2014, 136, 4544−4550

either goat anti-Oregon Green488 (Life Technologies, A-11095, 1:100, 10 μg/mL) or goat anti-biotin antibodies (Sigma-Aldrich, B3640, 1:300, 3.3 μg/mL) to enable imaging in the FITC channel. For detection of palmitoylated α-tubulin in Alexa488-clicked cells, cells were incubated with mouse anti-α-tubulin (Sigma-Aldrich, T9028, 1:800) overnight at 4 °C, washed with PBS-T, then incubated with rabbit anti-Alexa488 (Life Technologies, A-11094, 1:100, 10 μg/mL) for 1 h at room temperature. For detection of palmitoylated H-Ras, biotin-clicked cells were incubated with rabbit anti-H-Ras/K-Ras antibody (LSBio, LS-C165008, 1:5; since K-Ras is not palmitoylated, the click chemistry−proximity ligation assay detects palmitoylated H-Ras only) overnight at 4 °C, washed with PBS-T, then incubated for 1 h at room temperature with goat anti-biotin antibody (Sigma-Aldrich, B3640, 1:50, 20 μg/mL) to enable imaging in the FITC channel. Proximity ligation assay was performed with Duolink II reagents from Olink Bioscience.[26] Briefly, cells were washed with PBS-T and incubated with PLA probes (PLA probe minus and plus in blocking buffer, 1:5 dilution) for 1 h at 37 °C, then washed with PBS-T and subjected to ligation (1:5 dilution of ligation buffer and 1:40 dilution of ligase in water) for 30 min at 37 °C. After ligation, cells were washed with PBS-T and subjected to amplification with Detection Reagents Orange from Olink Bioscience (1:5 dilution of amplification stock and 1:80 dilution of polymerase in water) for 100 min at 37 °C. For detection of total α-tubulin or Shh, cells were stained with DyLight 405-conjugated secondary antibodies (1:500) for 30 min at room temperature after proximity ligation processing. To detect total palmitoylation in the palmitoylated H-Ras experiments, cells were stained with Alexa488-conjugated streptavidin (1:400) for 30 min at room temperature. Amplified samples on coverslips were washed with PBS-T then mounted with Duolink II Mounting Medium with or without DAPI. For 96-well plates, total H-Ras/K-Ras was detected with Alexa647-conjugated anti-rabbit secondary antibody (1:500, 30 min at room temperature). All samples in 96-well plates were incubated with Hoechst 33342 (5 μg/mL in PBS) for 10 min at room temperature, washed with PBS then stored in 100 μL PBS until imaging acquisition. All samples were protected from light.

Fluorescence Microscopy. Fluorescence images for samples on coverslips were captured on an upright LEICA SPE laser scanning confocal microscope (Leica Microsystems) and images were analyzed with Leica Application Suite Advanced Fluorescence (LAS AF) image processing software (Leica Microsystems) and Duolink ImageTool (Olink Bioscience). Fluorescence images for samples on 96-well plates were captured on a high throughput ImageXpress Micro imaging system (Molecular Devices) and images were analyzed by MetaXpress software (Molecular Devices). Spots representing palmitoylated Shh, α-tubulin, or H-Ras per cell were counted in Duolink ImageTool or MetaXpress software and reported as counts per cell (background threshold was selected based on the negative control samples).

■ ASSOCIATED CONTENT

Supporting Information

Optimization of fluorescence imaging of palmitoylated Hh, α-tubulin and H-Ras, effect of 2-bromopalmitic acid on palmitoylation of α-tubulin and the proteome, and 3D images (*z* sections) showing examples of colocalization of palmitoylated Hh, α-tubulin, and H-Ras with various cellular markers. This material is available free of charge via the Internet at http://pubs.acs.org.

■ AUTHOR INFORMATION

Corresponding Author

hannoush.rami@gene.com

Notes

The authors declare no competing financial interest.

■ ACKNOWLEDGMENTS

We thank Dr. Suzie Scales for helpful discussions and comments on the manuscript.

■ REFERENCES

(1) Rubin, L. L.; de Sauvage, F. J. *Nat. Rev. Drug Discovery* **2006**, *5*, 1026.
(2) Peukert, S.; Miller-Moslin, K. *ChemMedChem* **2010**, *5*, 500.
(3) Yauch, R. L.; Gould, S. E.; Scales, S. J.; Tang, T.; Tian, H.; Ahn, C. P.; Marshall, D.; Fu, L.; Januario, T.; Kallop, D.; Nannini-Pepe, M.; Kotkow, K.; Marsters, J. C.; Rubin, L. L.; de Sauvage, F. J. *Nature* **2008**, *455*, 406.
(4) Porter, J. A.; Young, K. E.; Beachy, P. A. *Science* **1996**, *274*, 255.
(5) Pepinsky, R. B.; Zeng, C.; Wen, D.; Rayhorn, P.; Baker, D. P.; Williams, K. P.; Bixler, S. A.; Ambrose, C. M.; Garber, E. A.; Miatkowski, K.; Taylor, F. R.; Wang, E. A.; Galdes, A. *J. Biol. Chem.* **1998**, *273*, 14037.
(6) Gao, X.; Arenas-Ramirez, N.; Scales, S. J.; Hannoush, R. N. *FEBS Lett.* **2011**, *585*, 2501.
(7) Heal, W. P.; Jovanovic, B.; Bessin, S.; Wright, M. H.; Magee, A. I.; Tate, E. W. *Chem. Commun.* **2011**, *47*, 4081.
(8) Weibrecht, I.; Leuchowius, K. J.; Clausson, C. M.; Conze, T.; Jarvius, M.; Howell, W. M.; Kamali-Moghaddam, M.; Soderberg, O. *Expert Rev. Proteomics* **2010**, *7*, 401.
(9) Zambito, A. M.; Wolff, J. *Biochem. Biophys. Res. Commun.* **1997**, *239*, 650.
(10) Caron, J. M. *Mol. Biol. Cell* **1997**, *8*, 621.
(11) Caron, J. M.; Herwood, M. *Chemotherapy* **2007**, *53*, 51.
(12) Zhao, Z.; Hou, J.; Xie, Z.; Deng, J.; Wang, X.; Chen, D.; Yang, F.; Gong, W. *Protein J.* **2010**, *29*, 531.
(13) Bhattacharyya, B.; Volff, J. *J. Biol. Chem.* **1975**, *250*, 7639.
(14) Wolff, J. *Biochim. Biophys. Acta* **2009**, *1788*, 1415.
(15) Zambito, A. M.; Wolff, J. *Biochem. Biophys. Res. Commun.* **2001**, *283*, 42.
(16) Linder, M. E.; Deschenes, R. J. *Nat. Rev. Mol. Cell Biol.* **2007**, *8*, 74.
(17) Eisenberg, S.; Laude, A. J.; Beckett, A. J.; Mageean, C. J.; Aran, V.; Hernandez-Valladares, M.; Henis, Y. I.; Prior, I. A. *Biochem. Soc. Trans.* **2013**, *41*, 79.
(18) Apolloni, A.; Prior, I. A.; Lindsay, M.; Parton, R. G.; Hancock, J. F. *Mol. Cell. Biol.* **2000**, *20*, 2475.
(19) Choy, E.; Chiu, V. K.; Silletti, J.; Feoktistov, M.; Morimoto, T.; Michaelson, D.; Ivanov, I. E.; Philips, M. R. *Cell* **1999**, *98*, 69.
(20) Goodwin, J. S.; Drake, K. R.; Rogers, C.; Wright, L.; Lippincott-Schwartz, J.; Philips, M. R.; Kenworthy, A. K. *J. Cell Biol.* **2005**, *170*, 261.
(21) Rocks, O.; Peyker, A.; Kahms, M.; Verveer, P. J.; Koerner, C.; Lumbierres, M.; Kuhlmann, J.; Waldmann, H.; Wittinghofer, A.; Bastiaens, P. I. *Science* **2005**, *307*, 1746.
(22) Misaki, R.; Morimatsu, M.; Uemura, T.; Waguri, S.; Miyoshi, E.; Taniguchi, N.; Matsuda, M.; Taguchi, T. *J. Cell Biol.* **2010**, *191*, 23.
(23) Hannoush, R. N.; Arenas-Ramirez, N. *ACS Chem. Biol.* **2009**, *4*, 581.
(24) Hannoush, R. N.; Sun, J. *Nat. Chem. Biol.* **2010**, *6*, 498.
(25) Wang, Q.; Chan, T. R.; Hilgraf, R.; Fokin, V. V.; Sharpless, K. B.; Finn, M. G. *J. Am. Chem. Soc.* **2003**, *125*, 3192.
(26) Soderberg, O.; Gullberg, M.; Jarvius, M.; Ridderstrale, K.; Leuchowius, K. J.; Jarvius, J.; Wester, K.; Hydbring, P.; Bahram, F.; Larsson, L. G.; Landegren, U. *Nat. Methods* **2006**, *3*, 995.
(27) Buglino, J. A.; Resh, M. D. *J. Biol. Chem.* **2008**, *283*, 22076.
(28) Gao, X.; Hannoush, R. N. *Nat. Chem. Biol.* **2014**, *10*, 61.